Chaos

Rössler-Network with time delay: Univariate impulse pinning synchronization

Kun Tian,[1] Hai-Peng Ren,[1, a)] and Celso Grebogi[1, 2]
[1)] *Shaanxi Key Laboratory of Complex System Control and Intelligent Information Processing, Xian University of Technology, Xian 710048, China*
[2)] *Institute for Complex System and Mathematical Biology, University of Aberdeen AB24 3UE, United Kingdom*

(Dated: 27 October 2020)

Rössler had a brilliant and successful life as a scientist, during which he published a benchmark dynamical system by using an electronic circuit interpreting chemical reactions. This is our contribution to honour his splendid erudite career. It is a hot topic to regulate a network behavior using the pinning control with respect to a small set of nodes in the network. Besides pinning to small number of nodes, small perturbation to the node dynamics is also demanded. In this paper, the pinning synchronization of coupled Rössler-Network with time delay using univariate impulse control is investigated. Using the Lyapunov theory, a theorem is proved for the asymptotic stability of synchronization in the network. Simulation is given to validate the correctness of the analysis and the effectiveness of the proposed univariate impulse pinning controller.

Keywords: Rössler-Network with time delay, univariate impulse control, pinning strategy, synchronization theorem.

Complex network synchronization has been an active research topic in the past two decades. It has attracted attention in engineering, physics, chemistry and biology. We consider in this work the impulse pinning control for network synchronization, which shows better application prospects in many fields. Many researchers considered fundamental issues associated with pinning control such as: (1) the controllability of complex networks by pinning control; (2) the minimum number of nodes that should be pinned; and (3) the coupling strength of the network that should be fixed to realize network synchronization. However, most existing works need to manipulate all state variables of the nodes, which is not possible to be implemented in systems containing an uncontrollable sub-system, such as the Rössler-Network with time delay. The univariate impulse pinning control for the synchronization of a complex network is a strategy to perturb the system at the inter-pulse interval, which is more energy efficient, requiring less perturbation to the original system. In this paper, a univariate impulse pinning synchronization method is proposed for the Rössler-Network. The asymptotic stability theory is rigorously proved for the network synchronization with univariate impulse pinning control. Our univariate impulse control is capable of dealing with a network having an uncontrollable sub-system, thus extending the applicability and relevance to a board range of disciplines.

I. INTRODUCTION

Complex networks are widely present in nature, ranging from ecosystems to infrastructure systems. In the past two decades, the synchronization of networks have been extensively studied in various pragmatic fields, such as communication[1,2], image processing[3,4] and biological systems[5]. Various useful control strategies have been proposed, such as pinning control[6], impulse control[7], distributed impulse control[8], and adaptive control[9].

As complex networks generally have large number of nodes in real world, it is unfeasible to manipulate all nodes simultaneously. Pinning method regulates a subset of the nodes to influence the dynamics of the whole network, which effectively reduces the number of required controllers. Grigoriev *et al*. presented the pinning control for the spatiotemporal chaos of a coupled map lattice[6]. Zhou *et al*. investigated how many nodes should be selected and how large the pinning strength should be to achieve network synchronization[10]. Recently, the impulse pinning synchronization research further combined the pinning strategy with impulse control for network synchronization[11]. By employing the pinning ratio, a novel pinning strategy was proposed to determine the node selection[12]. A mixed impulse pinning controller was proposed for the reaction-diffusion neural networks with time-varying and distributed delays[13]. Impulse pinning control was also proposed for stabilizing nonlinear dynamical networks with time-varying delay[14]. It was shown that the threshold on the coupling strength is a sufficient condition to guarantee the network synchronization by pinning control[15]. Pinning control is energy efficient, as it drives the full network to a desired state by manipulating a portion of the nodes. Impulse control is also energy-saving by manipulating the system in discrete times instead of continuous time. The impulse control can be constructed through an electronic circuit[16]. However, all existing research on impulse pinning con-

[a)] Electronic mail of corresponding author:renhaipeng@xaut.edu.cn

trol considers the regulation of all state variables. But in fact, some node dynamics contains state variables of an uncontrollable sub-system, such as in the Rössler system for describing chemical reactions. Therefore, it is of significance to investigate the controllers of the univariate pulse pinning synchronization of complex networks. Furthermore, it is desirable to use a minimum number of variables as possible.

Professor Otto E. Rössler proposed the Rössler system, lying an important foundation for experimental chaos theory. The Rössler system describes the characteristics of chemical kinetics. Moreover, Rössler defined hyperchaos, present in a four-dimensional flow having more than one positive Lyapunov exponents[17]. His contributions include elucidating the mechanism of labyrinth chaos, characterized by sensitive dependence on initial conditions, and flexible chaotic phase like chaotic walks[18]. Rössler system was widely studied as a paradigmatic chaotic system for research in different topics, like coupled oscillators synchronization[19], chemical reactions[20], and topological horseshoe[21].

As we have mentioned above, general impulse control methods manipulate all state variables of the system[22], which is not possible to use it for some application scenarios having an uncontrollable sub-system. Therefore, univariate impulsive control has a more practical significance than general impulse control. The univariate impulse synchronization for two hyperchaotic systems was proposed[16], which laid the theoretical foundation for the univariate impulse synchronization. However, univariate impulse control for a network becomes more challenging when combining with pinning control. Amid the mentioned references[11–15], two issues have been considered for impulse pinning control : (1) What is the coupling strength allowing synchronization of all nodes in the network? (2) How to select the pinned nodes for optimal control of the network? For the second issue, the maximum matching algorithm has been proposed, which identifies the maximum set of links that do not share starting or ending node. There are two methods to identify the maximum matching, including Hungarian algorithm[23] and Hopcrof-Karp algorithm[24]. We employ Hungarian algorithm in this work, whose underlying idea is to identify augmenting paths per iteration until there is no augmenting path with respect to the matching. However, it is difficult to simultaneously consider the relationship between the theoretical stability conditions of the univariate impulse controller and the pinning strategy. In this paper, we consider univariate impulse pinning control for the complex network, which may apply to the scenario in which some nodes and some node state variables cannot bear perturbations. A three-node network schematic diagram of the method is shown in Fig. 1. In Fig. 1, $\mathbf{x}$ represents the state vector of a single node, and x_u represents one controlled variable of the oscillator, and the x_i $(i = 1, 2, ..., m, i \neq u)$ represents the variables of the uncontrollable sub-system, m is the dimension of the node dynamics, and a_{21} and a_{31} represent the coupling. The external input signal u is the univariate controller imposed to the pinning node $\mathbf{x}_1$ in the network, it drives nodes $\mathbf{x}_2$ and $\mathbf{x}_3$ to synchronize with $\mathbf{x}_1$ indirectly.

The remainder of the paper is organized as follows. In Section II, the preliminaries of impulse differential equation are introduced. In Section III, the uniform asymptotic stability of univariate impulse control and the sufficient condition to achieve pinning synchronization are rigorously derived based on the Lyapunov stability theory. In Section IV, the simulation results are given to show the synchronization of two hyperchaotic Rössler-Network systems by the univariate impulse control, in order to demonstrate the feasibility and effectiveness of the proposed method. The conclusions are given in Section V.

II. PRELIMINARIES OF IMPULSE CONTROL DIFFERENTIAL EQUATION AND PINNING SYNCHRONIZATION OF COMPLEX NETWORK WITH TIME DELAY

Consider a general hyperchaotic network with time delay:

$$\dot{\mathbf{x}}_i(t) = \mathbf{B}\mathbf{x}_i(t) + \mathbf{D}f_1(\mathbf{x}_i(t)) + \mathbf{C}\mathbf{x}_i(t-\tau) + \sigma\sum_{j=1}^{N}\mathbf{A}\mathbf{H}(\mathbf{x}_j(t)), \tag{1}$$

where $\mathbf{x}_i(t) \in R^n$ represents the state vector of the i-th oscillator, $i = 1, 2, ..., N$, N is the number of oscillators in the network. σ is the coupling strength constant. $\mathbf{A} = (a_{ij})_{N\times N} \in R^{N\times N}$ stands for directed coupling matrix, where $a_{ij} = 1$, if there is a connection from node i to j, otherwise $a_{ij} = 0$ $(i \neq j)$, and $a_{ii} = 0$. $\mathbf{H}(\mathbf{x}_j) = \mathbf{x}_j - \mathbf{x}_i, \mathbf{H}(\mathbf{x}_j) \in R^n \to R^n$ is the internal coupling function among the oscillators in the network. $\mathbf{B}$, $\mathbf{C}$ are the parameters matrices. $f_1(\mathbf{x}_i(t)) : R_+ \times S(\rho) \to R^n$ are smooth nonlinear functions, where $R_+ = [0, +\infty)$. The time delay function used in this paper has a similar form as that proposed by Pyragas[25]. In fact, this work is also related to our past research on the time delay effect[26]. The time delay form is the same as that of Pyragas used to control chaos, while, we used the time delay to generate complex dynamics, including chaos. In conclusion, our investigation, together with Pyragas' work, shows that the time delay function is two-fold, like the sword has two edges, because one can use time delay to either suppress chaos or to generate chaos. This finding provides flexibility for control engineers to generate chaos when it is useful or to eliminate chaos when it is harmful just by tuning the controller parameters without altering the controller structure.

In this paper, we consider the network with univariate impulse pinning controllers. We wish to control the nodes in the network to synchronize with the leader node, meaning that the states of the other nodes are

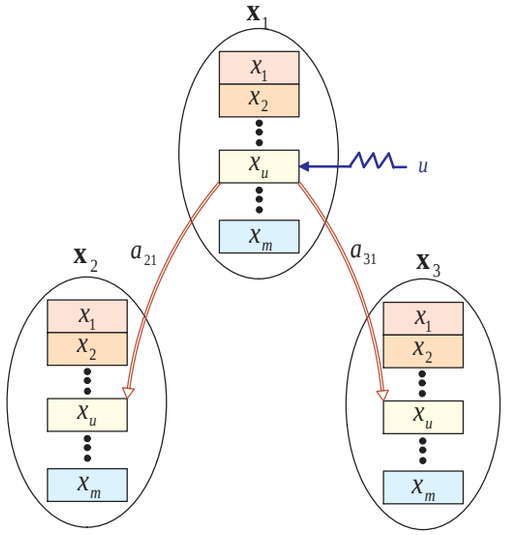

FIG. 1. Diagram of network with univariate control.

synchronized with the state of the leader node. It is defined that ℓ represents the number of pinning nodes, which are selected for manipulating the dynamics of the network. In general, we reorder the sequence of the nodes. Let $(i_1, i_2..., i_\ell)$ denotes the set of pinning nodes, and $(i_{\ell+1}, i_{\ell+2}..., i_N)$ denotes the set of the uncontrolled nodes. The individual node dynamics with univariate impulse pinning control is described by,

$$\begin{cases} \dot{\mathbf{x}}_i = \mathbf{B}\mathbf{x}_i + \mathbf{D}f_1(\mathbf{x}_i(t)) + \mathbf{C}\mathbf{x}_i(t-\tau) + \sigma\sum_{j=1}^{N}\mathbf{A}\mathbf{H}(\mathbf{x}_j), \\ \qquad\qquad\qquad\qquad\qquad\qquad t \neq t_k, \\ \Delta\mathbf{x}_i = \mathbf{x}_i(t_k^+) - \mathbf{x}_i(t_k^-) = \mathbf{C}_I(\mathbf{x}_i(t_k^-) - \mathbf{x}_\theta(t_k^-)), \\ \qquad\qquad\qquad\qquad\qquad 1 < i < \ell, t = t_k, \\ \Delta\mathbf{x}_i = 0, \qquad\qquad\qquad \ell+1 < i < N, t = t_k, \end{cases} \tag{2}$$

where $\mathbf{x}_\theta(t)$ represents the state of the leader oscillator, being the one node of the network that satisfies $\mathbf{x}_\theta \in \mathbf{x}_i (i = 1, ..., N)$. $\mathbf{C}_I$ is the undetermined impulse control matrix whose diagonal has only one nonzero element. The impulse time t_k satisfies $0 < t_0 < t_1 < t_2 < ...$ and $\lim_{k\to\infty} t_k = \infty$. $\Delta\mathbf{x}_i$ represents the "jump" states at the impulse time $t = t_k$, $\mathbf{x}_i(t_k^-) = \lim_{t\to t_k^-}\mathbf{x}_i(t)$ and $\mathbf{x}_i(t_k^+) = \lim_{t\to t_k^+}\mathbf{x}_i(t)$ represent the states at the left-hand and right-hand limits of time t_k, respectively.

Some preliminaries for the impulse differential equation are introduced next. We define some notation first[27]:

$K_1 = \{g \in C(R_+, R_+)\,|g(0) = 0, g(s) > 0, \forall s > 0\}$.

$K_2 = \{g \in C(R_+, R_+)|$ *is a non - decreasing function and* $g(0) = 0, g(s) > 0,$ for $s > 0\}$.

$S(\rho) = \{x \in R^n \,|\|x\| < \rho\}$, where $\|\cdot\|$ represents R^n space Euclidean norm;

$PC(D, F)$ denotes a piecewise continuous function from D to F.

Definition 1[27]: Let $V_0 = \{V : R_+ \times R_+^n \to R_+\}, V \in V_0$, for $[t, x(t)] \in [nT, (n+1)T] \times R_+^n$. The upper right derivative of $V(t, \mathbf{x}(t))$ is defined as $D^+V[t, \mathbf{x}(t)] = \lim_{h\to 0^+}\sup\frac{1}{h}\{V[t+h, \mathbf{x}(t) + hf(t, \mathbf{x}(t))] - V(t, \mathbf{x}(t))\}$.

Lemma 1[27]: Assume that $a_k, b_k, c_k \in K_1$, $g \in K_2$, $p \in PC(R_+, R_+)$, and $V : [-r, \infty] \times S(\rho) \to R_+$, where V is continuous on $(-r, t_0] \times S(\rho)$ and $(t_{k-1}, t_k] \times S(\rho)$, $k = 1, 2, ...,$ for each $x \in S(\rho)$, and $k = 0, 1, 2, ...,$ $\lim_{(t,y)\to(t_k^-,x)} V(t, y) = V(t_k^-, x)$ exists; if V is locally Lipschitz in x and the following conditions hold:

(1) $b_k(|\mathbf{x}|) \leqslant V(t, \mathbf{x}) \leqslant a_k(|\mathbf{x}|), (t, x) \in [-r, \infty) \times S(\rho)$;

(2) $D^+V(t, \phi(0)) \leqslant p(t)c_k[V(t, \phi(0))]$, for all $t \neq t_k$ in R_+, and $\phi \in PC([-r, 0], S(\rho))$ whenever $V(t, \phi(0)) \geqslant g[V(t + s, \phi(s))]$ for $s \in [-r, 0]$.

(3) $V(t_k, \phi(0) + I_k) \leqslant g\left[V\left(t_k^-, \phi(0)\right)\right]$ for all $(t_k, \phi) \in R_+ \times PC([-r, 0], S(\rho_1))$ for $\phi(0^-) = \phi(0)$.

(4) $\Delta = \sup_{k\in z}\{\tau_k - \tau_{k-1}\} < \infty$, where Δ is the impulse interval, and $M_1 = \sup_{t>0}\int_t^{t+\Delta} p(s)ds < \infty$, $M_2 = \inf_{q>0}\int_{g(q)}^{q}\frac{ds}{c(s)} > M_1$.

Then, the trivial solution of system (2) is uniformly asymptotically stable.

III. HYPERCHAOTIC NETWORK SYNCHRONIZATION USING UNIVARIATE IMPULSE PINNING CONTROL

This work aims at synchronizing all oscillators with the leader oscillator by constructing suitable univariate impulse pinning controllers. If one wishes to control a network with the pinned nodes, the controllability condition, referred to as Kalman's controllability rank condition, must be satisfied. However, for a higher order nonlinear node system, it is hardly possible to build the Kalman matrix straightforwardly. In fact, the controllability of the nonlinear system does not depend on the rank, but it depends on the system structure, e.g., the input vector[28]. This means that the same system state matrix, but different input vector, leads to different controllability. Therefore, we present that the network is controllable when the two conditions are satisfied: (1) the node system is controllable; and (2) the topology structure is controllable. According to Aguirre and Letellier[28], a nonlinear system can be written as $\dot{\mathbf{x}} = \mathbf{f}(\mathbf{x}) + \mathbf{C}_I\mathbf{u}$, where $\mathbf{f}(\mathbf{x})$ is the nonlinear state equation, $\mathbf{C}_I$ is input matrix. The controllability matrix of the system is $\Theta(\mathbf{x}) = [\, ad_{\mathbf{f}}^0\mathbf{C}_I \;\; ad_{\mathbf{f}}^1\mathbf{C}_I \;\; \cdots \;\; ad_{\mathbf{f}}^{s+2}\mathbf{C}_I \,]$, where the Lie bracket

and the recursion relation are $ad_{\mathbf{f}}\mathbf{C}_I = [\mathbf{f}, \mathbf{C}_I] = \frac{\partial \mathbf{C}_I}{\partial \mathbf{x}} \cdot \mathbf{f} - \frac{\partial \mathbf{f}}{\partial \mathbf{x}} \cdot \mathbf{C}_I$, $ad^k_{\mathbf{f}}\mathbf{C}_I = [\mathbf{f}, ad^{k-1}_{\mathbf{f}}\mathbf{C}_I], k \geqslant 1$, and $ad^0_{\mathbf{f}}\mathbf{C}_I = \mathbf{C}_I$. The system is said to be controllable if the matrix $\Theta(\mathbf{x})$ has full row rank[28]. The error dynamics network is said to be controllable if $\mathbf{Q} = \left[\mathbf{G}, \mathbf{AG}, \mathbf{A^2G}, ..., \mathbf{A^{N-1}G}\right]$ is full rank[29], where $\mathbf{G}$ is the $N \times \ell$ input matrix corresponding to the selected pinning nodes. It is worth noting that the controllability condition can also be applied to decide the controllability of the topology structure with nonlinear nodes networks[29,30]. The determination of the number ℓ of pinning nodes is a key point. In general, we increase the number of pinning nodes from 1, set its position (putting into which state variables), and then check the controllability matrix rank. If it is full rank, the pinning node(s) can be selected as an option. Else, we continue the procedure by changing the position of the state variable for pinning, checking the rank again, until all positions of the variables are tried. If all positions are tried and we cannot obtain a full rank matrix, then we have to increase the pinning node number to 2, and so on. This procedure is illustrated by the flowchart given in Fig. 2. After that, we state and prove a uniform asymptotic stability theorem for the error dynamics network. In the following, we reorder the sequence of the nodes, i.e., $i_1, ..., i_\ell$ represents the pinning nodes and others are uncontrolled nodes. Importantly, our stability Theorem 1 is independent of the Hungarian algorithm.

Let the θ-th oscillator in the network be considered as leader, described as,

$$\dot{\mathbf{x}}_\theta(t) = \mathbf{B}\mathbf{x}_\theta(t) + \mathbf{D}f_1(\mathbf{x}_\theta(t)) + \mathbf{C}\mathbf{x}_\theta(t-\tau) + \sigma\sum_{i=1}^{N} a_{in}(\mathbf{x}_i(t) - \mathbf{x}_\theta(t)), \tag{3}$$

where a_{in} is the connection between the leader node and other nodes.

From the drive node in Eq. (3) and the response nodes in Eq. (1), we define the error as $\mathbf{e}_i(t) = \mathbf{x}_i(t) - \mathbf{x}_\theta(t), (i = 1, 2, ..., N)$. The error dynamics network is given by the following,

$$\dot{\mathbf{e}}_i(t) = \mathbf{B}\mathbf{e}_i(t) + \mathbf{D}\tilde{f}_1(\mathbf{e}_i) + \mathbf{C}\tilde{f}_2(\mathbf{e}_i(t-\tau)) + \sigma\sum_{j=1}^{N} \tilde{\mathbf{A}}\mathbf{H}(e_j(t)), \tag{4}$$

where $\tilde{f}_1(\mathbf{e}_i) = f_1(\mathbf{x}_i(t)) - f_1(\mathbf{x}_\theta(t))$, $\tilde{f}_2(\mathbf{e}_i(t-\tau)) = \mathbf{x}_i(t-\tau) - \mathbf{x}_\theta(t-\tau)$. $\tilde{\mathbf{A}}$ is a singular matrix.

The objective is to design a controller $\mathbf{u}_i$ such that the error dynamics network (4) is asymptotically stable at origin, i.e., $\mathbf{e}_i = 0$ for all i. The univariate impulse pinning controller is given as follows,

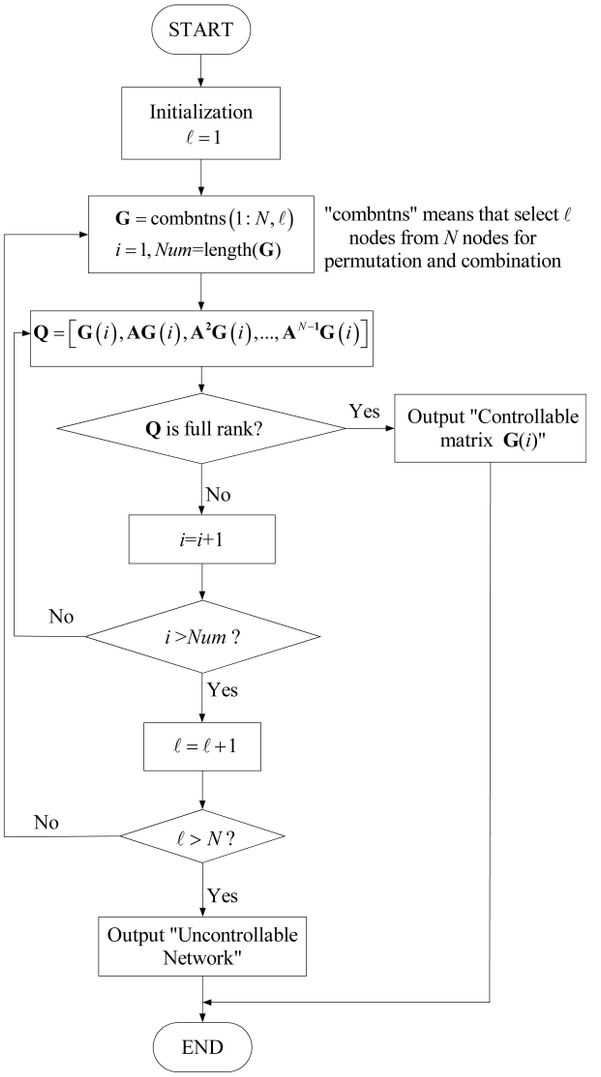

FIG. 2. The flowchart to determine the pinning nodes.

$$\begin{cases} \mathbf{u}_i(t) = \mathbf{C}_I\mathbf{e}_i(t_k^-), 1 < i < \ell, \ t = t_k, \\ \mathbf{u}_i(t) = 0, \ \ell + 1 < i < N, \ t = t_k, \\ \mathbf{u}_i(t) = 0, \ 1 < i < N \ , \ t \neq t_k \ , \end{cases} \tag{5}$$

where $\mathbf{C}_I$ ($\mathbf{C}_I = diag(0, ..., c, 0, ...)$ represents the impulse control matrix. The location of c in the diagonal matrix is determined by the controllability and observability of the system. The basic principle is that the impulse control is operated on the observable available in the state equation[31,32]. With the univariate impulse pinning controller (5), the error dynamics network can be described as follows:

$$\begin{cases} \dot{\mathbf{e}}_i(t) = \mathbf{B}\mathbf{e}_i(t) + \mathbf{D}\tilde{f}_1(\mathbf{e}_i) + \mathbf{C}\tilde{f}_2(\mathbf{e}_i(t-\tau)) + \sigma\sum_{j=1}^{N}\tilde{\mathbf{A}}\mathbf{H}(e_j(t)), \\ \qquad\qquad\qquad\qquad\qquad\qquad\qquad\qquad t \neq t_k, \\ \Delta\mathbf{e}_i(t_k) = \mathbf{C}_I\mathbf{e}_i(t_k^-), \qquad\qquad 1 < i < \ell, t = t_k, \\ \Delta\mathbf{e}_i(t_k) = 0, \qquad\qquad\qquad \ell+1 < i < N, t = t_k, \end{cases} \tag{6}$$

Next, we rewrite network (1) as,

$$\begin{cases} \dot{\mathbf{x}}_i = B_1\mathbf{x}_i + D_1 f_{1x}(\mathbf{x}_i(t), y_i(t)) + C_1\mathbf{x}_i(t-\tau), \\ \dot{y}_i = B_2 y_i + D_2 f_{1y}(\mathbf{x}_i(t), y_i(t)) + C_2 y_i(t-\tau) \\ \qquad + \sigma\sum_{i=1}^{N} A_{ij}H(y_j), \end{cases} \tag{7}$$

where $\mathbf{x}_i$ represents the state variables of uncontrollable sub-system of node i, and y_i is the state variable of controllable sub-system of node i. Therefore, in Eq. (6), we have $\mathbf{e}_i(t) = [\mathbf{e}_{\mathbf{x}_i}(t), e_{y_i}(t)]^T$

Theorem 1 Considering system (6) to satisfy the following two conditions:

(1) There exist constants l_1 and l_2 yielding $\|f_{1x}(\mathbf{x}_i, y_i)\|^2 \leqslant l_1\|(\mathbf{x}_i, y_i)\|^2$ and $\|f_{1y}(\mathbf{x}_i, y_i)\|^2 \leqslant l_2\|(\mathbf{x}_i, y_i)\|^2$,
(2) $M = \max\left\{2\left(\lambda_{\max}(B_1^T) + \sqrt{\lambda_{\max}(D_1^T D_1)}l_1 + \frac{1}{2} + \frac{l_1^2\|C_1\|^2}{2c^2}\right),\right.$
$\left. 2\left(\lambda_{\max}(B_2) + \sqrt{\lambda_{\max}(D_2^T D_2)}l_2 + \frac{1}{2} + \frac{l_2^2\|C_2\|^2}{2c^2}\right)\right\}$,
$0 < \Delta < -\frac{\ln\left((1+c)^2\delta + 1 - \delta\right)}{M}$,
where $\lambda_{\max}(\cdot)$ is the maximum eigenvalue of the matrix in brackets and Δ is the impulse interval, δ is the pinning ratio defined as $\delta = \ell/N$. Then the error dynamics network (6) is uniformly asymptotically stable.

In this sense, the oscillators of the complex dynamical network, given by Eq. (1), can be driven to synchronize with the leader oscillator by univariate impulse controllers.

Proof of Theorem 1

Select Lyapunov function candidate as:

$$V = \sum_{i=1}^{N} {\mathbf{e}_i}^T \mathbf{P}\mathbf{e}_i \tag{8}$$

For $t = t_k$:

$$\begin{aligned} &V(t_k, e_i(t_k^+)) = \sum_{i=1}^{N}\mathbf{e}_i^T(t_k)P\mathbf{e}_i(t_k) \\ &= \sum_{i=1}^{\ell}\mathbf{e}_{x_i}^T(t_k)P\mathbf{e}_{x_i}(t_k) + \sum_{i=1}^{\ell}e_{y_i}^T(t_k)Pe_{y_i}(t_k) + \sum_{i=\ell+1}^{N}\mathbf{e}_{x_i}^T(t_k)P\mathbf{e}_{x_i}(t_k) + \sum_{i=\ell+1}^{N}e_{y_i}^T(t_k)Pe_{y_i}(t_k) \\ &= \sum_{i=1}^{\ell}e_{x_i}^T(t_k^-)Pe_{x_i}(t_k^-) + (1+c)^2\sum_{i=1}^{\ell}e_{y_i}^T(t_k^-)Pe_{y_i}(t_k^-) + \sum_{i=\ell+1}^{N}e_{x_i}^T(t_k^-)Pe_{x_i}(t_k^-) + \sum_{i=\ell+1}^{N}e_{y_i}^T(t_k^-)Pe_{y_i}(t_k^-) \\ &\leqslant (1+c)^2\delta\sum_{i=1}^{N}e_i^T(t_k^-)Pe_i(t_k^-) + (1-\delta)\sum_{i=1}^{N}e_i^T(t_k^-)Pe_i(t_k^-) \\ &\leqslant \left((1+c)^2\delta + 1 - \delta\right)V(t_k^-, e_i(t_k^-)) \\ &= g(V(t_k^-, e_i(t_k^-))), \end{aligned} \tag{9}$$

where $g(V) = \left((1+c)^2\delta + 1 - \delta\right)\cdot V$.

The derivative of $V(t)$ yields,

$$\begin{aligned} &D^+V(t, \mathbf{e}(t)) = 2\left(\sum_{i=1}^{N}\dot{e}_{x_i}^T(t)e_{x_i}(t) + \sum_{i=1}^{N}e_{y_i}^T(t)\dot{e}_{y_i}(t)\right) \\ &= 2\left[\sum_{i=1}^{N}(e_{x_i}^T B_1^T + \tilde{f}_{1x}^T D_1^T + C_1\tilde{f}_{2x}(e_{x_i}(t-\tau)))e_{x_i} + \sum_{i=1}^{N}e_{y_i}^T(B_2 e_{y_i} + D_2\tilde{f}_{1y} + C_2\tilde{f}_{2y}(e_{y_i}(t-\tau)) - \sigma\sum_{j=1,j\neq n}^{N}\tilde{A}_{ij}H(e_j))\right] \\ &\leqslant 2\lambda_{\max}(B_1^T)\sum_{i=1}^{N}e_{x_i}^T e_{x_i} + 2\lambda_{\max}(B_2)\sum_{i=1}^{N}e_{y_i}^T e_{y_i} + 2\sum_{i=1}^{N}\tilde{f}_{1x}^T D_1^T e_{x_i} + 2\sum_{i=1}^{N}e_{y_i}^T D_2\tilde{f}_{1y} \\ &+ 2\sum_{i=1}^{N}C_1\tilde{f}_{2x}(e_{x_i}(t-\tau))e_{x_i} + 2\sum_{i=1}^{N}e_{y_i}^T C_2\tilde{f}_{2y}(e_{y_i}(t-\tau)) - 2\sigma\sum_{i=1}^{N}\sum_{j=1,j\neq n}^{N}e_{y_i}^T\tilde{A}_{ij}H(e_j). \end{aligned} \tag{10}$$

We have

$$\begin{aligned}
&2\sum_{i=1}^{N}\tilde{f}_{1x}D_1^T e_{x_i}^T \leqslant 2\sum_{i=1}^{N}\left(\sqrt{\left\|\tilde{f}_{1x}D_1^T\right\|^2}\cdot\left\|e_{x_i}^T\right\|\right)\\
&\leqslant 2\sum_{i=1}^{N}\left(\sqrt{\lambda_{\max}(D_1^T D_1)l_1^2\|e_{x_i}\|^2}\cdot\left\|e_{x_i}^T\right\|\right)\\
&\leqslant 2\sqrt{\lambda_{\max}(D_1^T D_1)}l_1\sum_{i=1}^{N}e_{x_i}e_{x_i}^T.
\end{aligned}\tag{11}$$

Similarly with Eq. (11), we have,

$$2\sum_{i=1}^{N}e_{y_i}^T D_2^T\tilde{f}_{1y}\leqslant 2\sqrt{\lambda_{\max}(D_2^T D_2)}l_2\sum_{i=1}^{N}e_{y_i}^T e_{y_i}.\tag{12}$$

$$\begin{aligned}
&2\sum_{i=1}^{N}e_{y_i}^T C_2\tilde{f}_{2y}(e_{y_i}(t-\tau))\leqslant\sum_{i=1}^{N}\left(\left\|e_{y_i}^T\right\|^2+\|C_2\|^2\cdot l_2^2\|e_{y_i}(t-\tau)\|^2\right)\\
&\leqslant\left(1+\frac{l_2^2\|C_2\|^2}{c^2}\right)\sum_{i=1}^{N}e_{y_i}e_{y_i}^T.
\end{aligned}\tag{13}$$

Similarly with Eq. (13), we have,

$$2\sum_{i=1}^{N}C_1\tilde{f}_{2x}(e_{x_i}(t-\tau))e_{x_i}\leqslant\left(1+\frac{l_1^2\|C_1\|^2}{c^2}\right)\sum_{i=1}^{N}e_{x_i}e_{x_i}^T.\tag{14}$$

Let $\sum_1 = diag[\underbrace{1,...,1}_{\ell},\underbrace{0,...,0}_{N-\ell}]$ denotes the diagonal matrix corresponding to the pinning node.

Note that the row vector of coupling matrix $A_{nj}=0$, we get,

$$\begin{aligned}
&2\sigma\sum_{i=1}^{N}\sum_{j=1,j\neq n}^{N}e_{y_i}^T\tilde{A}_{ij}H(e_j)\\
&=2\sigma\delta\sum_{i=1}^{l}\sum_{j=1,j\neq n}^{l}e_{y_i}^T\sum\nolimits_1\tilde{A}_{ij}H(e_j)\\
&\leqslant 0.
\end{aligned}\tag{15}$$

From Eqs. (11)-(15), we have,

$$\begin{aligned}
D^+V(t,\mathbf{e}(t))&\leqslant 2\lambda_{\max}(B_1^T)\sum_{i=1}^{N}e_{x_i}^T e_{x_i}+2\lambda_{\max}(B_2)\sum_{i=1}^{N}e_{y_i}^T e_{y_i}+2\sqrt{\lambda_{\max}(D^T D)}l_1\sum_{i=1}^{N}e_{x_i}e_{x_i}^T\\
&+2\sqrt{\lambda_{\max}(D^T D)}l_2\sum_{i=1}^{N}e_{y_i}^T e_{y_i}+\left(1+\tfrac{l_2^2\|C_2\|^2}{c^2}\right)\sum_{i=1}^{N}e_{y_i}e_{y_i}^T+\left(1+\tfrac{l_1^2\|C_1\|^2}{c^2}\right)\sum_{i=1}^{N}e_{x_i}e_{x_i}^T\\
&\leqslant 2\left(\lambda_{\max}(B_1^T)+\sqrt{\lambda_{\max}(D_1^T D_1)}l_1+\tfrac{1}{2}+\tfrac{l_1^2\|C_1\|^2}{2c^2}\right)\sum_{i=1}^{N}e_{x_i}^T e_{x_i}\\
&+2\left(\lambda_{\max}(B_2)+\sqrt{\lambda_{\max}(D_2^T D_2)}l_2+\tfrac{1}{2}+\tfrac{l_2^2\|C_2\|^2}{2c^2}\right)\sum_{i=1}^{N}e_{y_i}e_{y_i}^T\\
&\leqslant p(t)V(t,\mathbf{e}(t)),
\end{aligned}\tag{16}$$

where $p(t)=\max\left\{2\left(\lambda_{\max}(B_1^T)+\sqrt{\lambda_{\max}(D_1^T D_1)}l_1+\frac{1}{2}+\frac{l_1^2\|C_1\|^2}{2c^2}\right),\right.$
$\left.2\left(\lambda_{\max}(B_2)+\sqrt{\lambda_{\max}(D_2^T D_2)}l_2+\frac{1}{2}+\frac{l_2^2\|C_2\|^2}{2c^2}\right)\right\}$.

Assuming that $c(s)=s, M=p(t)$, and from the condition (4) of Lemma 1, we have

$$\begin{aligned}
M_2-M_1&=\inf_{q>0}\int_{g(q)}^{q}\frac{ds}{c(s)}-\sup_{t>0}\int_{t}^{t+\Delta}p(s)ds\\
&=\ln q-\ln g(q)-M\cdot\Delta\\
&=-\ln g-M\cdot\Delta>0.
\end{aligned}\tag{17}$$

According to Eq. (17), we obtain the following condition for impulse interval Δ,

$$0<\Delta<-\frac{\ln\left((1+c)^2\delta+1-\delta\right)}{M},\tag{18}$$

where $M=\max\left\{2\left(\lambda_{\max}(B_1^T)+\sqrt{\lambda_{\max}(D_1^T D_1)}l_1+\frac{1}{2}+\frac{l_1^2\|C_1\|^2}{2c^2}\right),\right.$
$\left.2\left(\lambda_{\max}(B_2)+\sqrt{\lambda_{\max}(D_2^T D_2)}l_2+\frac{1}{2}+\frac{l_2^2\|C_2\|^2}{2c^2}\right)\right\}$.

Therefore, the error dynamics network (6) is asymptotically stable.

End of proof.

IV. NUMERICAL SIMULATIONS

Consider the Rössler system with time delay network given by:

$$\begin{cases} \dot{x}_i = -y_i - z_i + K(x_i(t-\tau) - x_i(t)), \\ \dot{y}_i = x_i + a y_i + \sigma \sum_{j=1}^{N} a_{ij}(y_j - y_i), \\ \dot{z}_i = b + z_i(x_i - \bar{c}), \end{cases} \tag{19}$$

where $x_i, y_i, z_i \in R^n$ represents the state variables of the oscillator i $(i = 1, 2, ..., N)$. The parameters are $a = b = 0.1, \bar{c} = 1.5$, $K = 10.5, \tau = 1$. This node dynamics with time delay is hyperchaotic[16]. We consider directed random network with $N = 10$, $\sigma = 0.025$, and the directed small-world network with $N = 30$, $\sigma = 0.23$ in the simulations. The topology connection diagram of two different networks is shown in Fig. 3(a) and Fig. 3(d), respectively. The node oscillator exhibits a chaotic attractor, as shown in the Fig. 4. In this work, the variable y of system (19) is a controlled variable, corresponding to x_u in Fig. 1.

We first derive the controllability of Rössler system with time delay. We expand the function of the system with the time-lag units of $s + 3$ dimensions[33], as shown in (20).

$$\begin{cases} \dot{x} = -y - z + K(u_s - u_1) \\ \dot{y} = x + ay \\ \dot{z} = b + z(x - c) \\ u_1 = \frac{\alpha x - u_1}{T} \\ u_2 = \frac{u_1 - u_2}{T} \\ u_3 = \frac{u_2 - u_3}{T} \\ u_4 = \frac{u_3 - u_4}{T} \\ \vdots \\ u_s = \frac{u_{s-1} - u_s}{T} \end{cases}, \tag{20}$$

where $T = \tau/s$, τ is time delay, s is the number of time-lag units cascade, α is the compensation gain of the time-lag units. When T is small enough, the time-lag unit approximates as a pure delay. In this work, we only investigate the controller using y as manipulated variable. Therefore, the input vector field $\mathbf{C}_I$ is given by $\mathbf{C}_I = \begin{bmatrix} 0 \\ 1 \\ 0 \\ \vdots \\ 0 \end{bmatrix}_{(s+3)\times(1)}$. The partial derivative of the system matrix is given by

$$\frac{\partial f}{\partial \mathbf{x}} = \begin{bmatrix} -K & -1 & -1 & 0 & 0 & \cdots & 0 & 0 & K \\ 1 & a & 0 & 0 & 0 & \cdots & 0 & 0 & 0 \\ z & 0 & x-c & 0 & 0 & 0 & \cdots & 0 & 0 \\ \alpha/T & 0 & 0 & -1/T & 0 & 0 & \cdots & 0 & 0 \\ 0 & 0 & 0 & 1/T & -1/T & 0 & \cdots & 0 & 0 \\ 0 & 0 & 0 & 0 & 1/T & -1/T & 0 & \cdots & 0 \\ \vdots & \vdots & \vdots & \vdots & \vdots & \vdots & \vdots & \vdots & \vdots \\ \vdots & \vdots & \vdots & \vdots & \vdots & \vdots & \vdots & \vdots & \vdots \\ 0 & 0 & 0 & 0 & 0 & \cdots & 0 & 1/T & -1/T \end{bmatrix}_{(s+3)\times(s+3)} \tag{21}$$

The controllability matrix for the system, Eq. (20), is

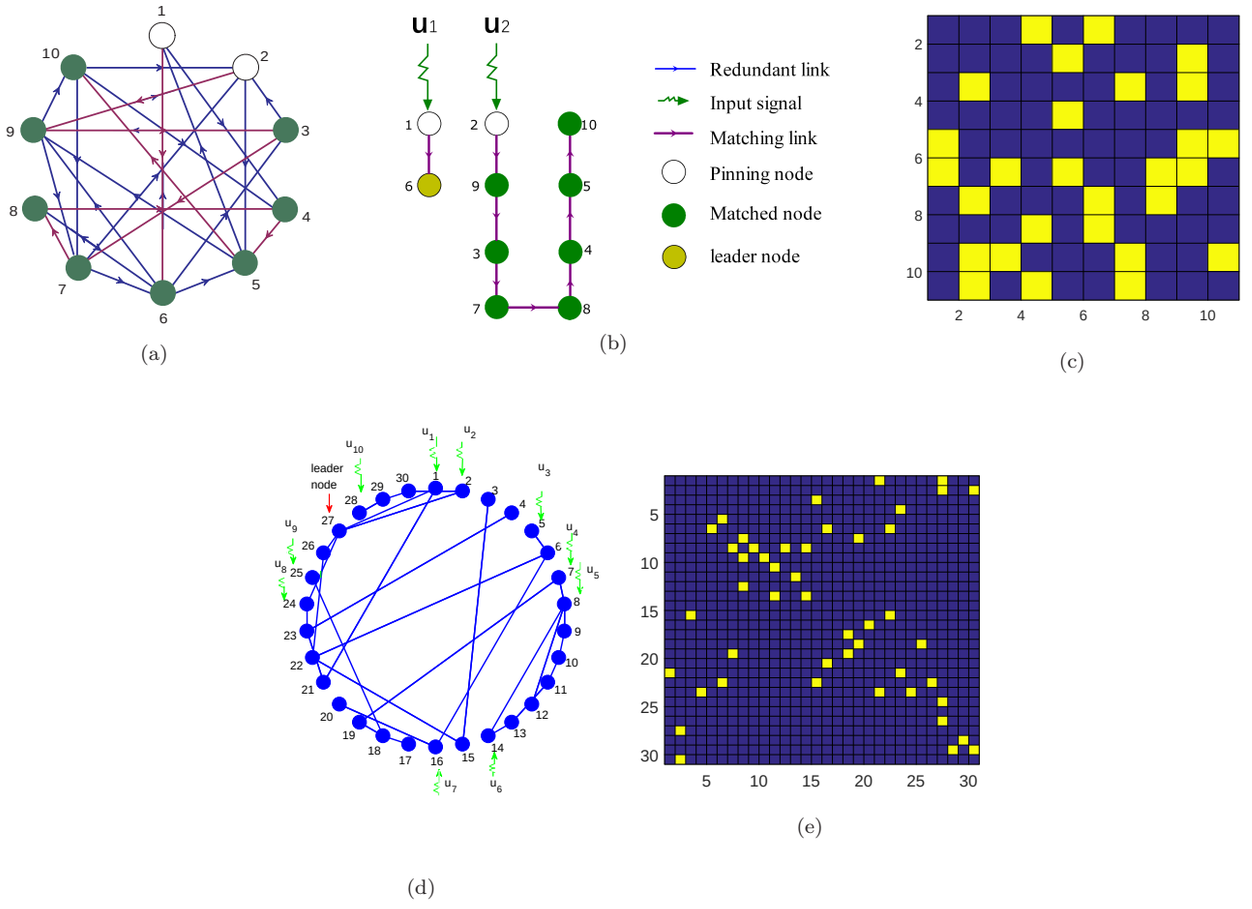

FIG. 3. Rössler-Network topology with node dynamics given by a Rössler system. (a) 10-node directed random network topology; (b) maximum matching of directed path, where pinning nodes are shown in blank; (c) connection matrix of the network in (a) (different color represents different connection weights: 0-blue lattice; 1-yellow lattice); (d) 30-node directed small world network topology, where the pinning nodes are marked by green arrow $\mathbf{u} = (u_1, u_2, ..., u_{11})^T$; (e) connection matrix of the network in (d) (0-blue lattice; 1-yellow lattice).

$$\Theta(\mathbf{x}) = \begin{bmatrix} 0 & 1 & K-a & K(K-a)+a^2-z-1 & * & * & * & * & * & * & * & * \\ 1 & -a & a^2-1 & 2a-K-a^3 & * & * & * & * & * & * & * & * \\ & & -z & -b-zK+az & * & * & * & * & * & * & * & * \\ & & -\alpha/T & [-\alpha T(K-a)-\alpha]/T^2 & * & * & * & * & * & * & * & * \\ & & & -\alpha/T^2 & [\alpha(K-a+2T)]/T^2 & * & * & * & * & * & * & * \\ & & & & -\alpha/T^3 & * & * & * & * & * & * & * \\ & & & & & -\alpha/T^4 & * & * & * & * & * & * \\ & & & & & & -\alpha/T^5 & * & * & * & * & * \\ & & & & & & & \ddots & * & * & * & * \\ & & & & & & & & \ddots & * & * & * \\ & & & & & & & & & \ddots & * & * \\ & & & & & & & & & & -\alpha/T^s & * \end{bmatrix}. \quad (22)$$

Thus, the controllability matrix $\Theta(\mathbf{x})$ has full row rank, meaning that the system is controllable. Next, we discuss the controllability of the topology. The network is said to be controllable when the matrix $\mathbf{Q} = [\mathbf{G}, \mathbf{AG}, \mathbf{A^2G}, ..., \mathbf{A^{N-1}G}]$ is full rank, according to the reference 29. Based on the two conditions above, the network is controllable.

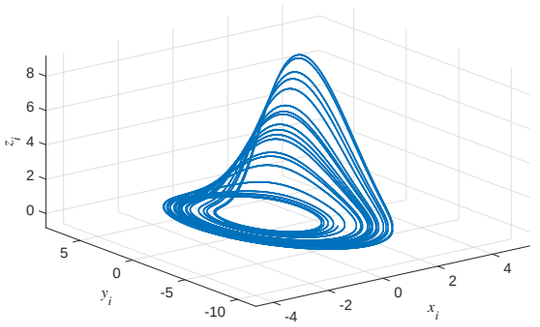

FIG. 4. Chaotic attractor of the i-th Rössler oscillator with time delay in the random network.

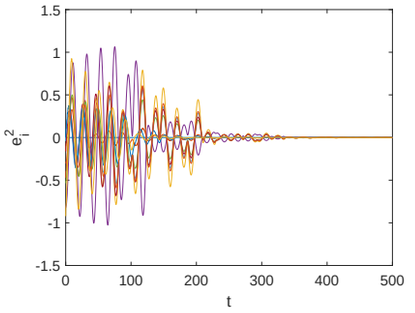

FIG. 5. Synchronization errors e_i^2 of the network in Fig. 1(a) (10-node directed random network), when the univariate impulse pinning control is active at $t = 100s$.

A. Simulation results

We consider the individual node oscillator of the Rössler-Network, Eq. (19), in this paper. We assume that $(X_i^*,\ Y_i^*,\ Z_i^*)$ is the equilibrium of Rössler oscillator, where $X_i^* = -aY_i^*$, $Z_i^* = -Y_i^*$, $aY_i^{*2} + \bar{c}Y_i^* + b = 0$. We define $X_i = x_i - X_i^*$, $Y_i = y_i - Y_i^*$, $Z_i = z_i - Z_i^*$ and the transformation as given in Eq. (23),

$$\begin{aligned}\dot{Z}_i &= b + x_i z_i - \bar{c} z_i \\ &= b + (X_i - aY_i^*)(Z_i - Y_i^*) - \bar{c}(Z_i - Y_i^*) \\ &= X_i Z_i - X_i Y_i^* - aZ_i Y_i^* - \bar{c} Z_i \\ &= X_i Z_i + X_i Z_i^* + Z_i(X_i^* - \bar{c}).\end{aligned} \tag{23}$$

We then obtain the following transformation of Eq. (19), as shown in Eq. (24),

$$\begin{cases}\dot{X}_i = -Y_i - Z_i + K(X_i(t-\tau) - X_i), \\ \dot{Y}_i = X_i + aY_i + \sigma \sum_{j=1}^{N} a_{ij}(Y_j - Y_i), \\ \dot{Z}_i = X_i Z_i + X_i Z_i^* + Z_i(X_i^* - \bar{c}),\end{cases} \tag{24}$$

where $B_1 = \begin{bmatrix} -K & -1 \\ Z_i^* & X_i^* - \bar{c} \end{bmatrix}$, $D_1 = \begin{bmatrix} 1 \\ 1 \end{bmatrix}$, $C_1 = \begin{bmatrix} K \\ 0 \end{bmatrix}$, $f_{x_i} = \begin{bmatrix} -Y_i \\ X_i Z_i \end{bmatrix}$, $B_2 = a$, $D_2 = 1$, $f_{y_i} = X_i$, $C_2 = 0$, in the form of Eq. (7) with $\mathbf{x} = [X_i, Z_i]^T$, $y = Y_i$. As learned from the above form, the system is decomposed into two subsystems, namely, B_1 and B_2. There are two equilibria $(X_i^*, Y_i^*, Z_i^*)_{1,2} = (0.0007, -0.007, 0.007), (0.1493, -1.493, 1.493)$ in the oscillator. It happens that the eigenvalues of B_1 have negative real part and the eigenvalues of B_2 is decided by the parameter a. Consequently, for each Rössler oscillator in the network, subsystem B_1 consisting of the variables x and z is stable. We know that the variable y is an observable state, then one can apply state feedback to control state y in order to achieve the network synchronization.

Let the node $\mathbf{X}_\theta(t)$ be the leader node, so we have the error $e_i^1 = X_i - X_\theta$, $e_i^2 = Y_i - Y_\theta$, $e_i^3 = Z_i - Z_\theta$. The impulse control gain is $c = -1.9$. For the network in Fig. 3(a), the procedure in Fig. 2 for calculating pinning nodes could be replaced by the maximum matching. The result is shown in Fig. 3(b), which indicates the two matching paths, starting from unmatched nodes 1 and 2 (blank nodes in Fig. 3(b)), ending at the matched nodes 6 and 10 (green nodes in Fig. 3(b)), respectively. The unmatched nodes are the minimal set of the number of required external controllers. The control link starts from an unmatched node in a directed path and ends at the end of the matching path. Therefore, controllers on the nodes $\mathbf{X}_1$ and $\mathbf{X}_2$ can exert full control. It is verified that if one chooses the controllers on $\mathbf{X}_1$ and $\mathbf{X}_2$, the controllability matrix $\mathbf{Q}$ is full rank. For the network in Fig. 3(d), the pinning nodes are $\mathbf{X}_1, \mathbf{X}_2, \mathbf{X}_5, \mathbf{X}_7, \mathbf{X}_8, \mathbf{X}_{14}, \mathbf{X}_{16}, \mathbf{X}_{24}, \mathbf{X}_{25}$, and $\mathbf{X}_{28}$ (see green arrows in Fig. 3(d)), that satisfies the controllability matrix $rank(\mathbf{Q}) = N$. We pin the mentioned two nodes in Fig. 3(a) and eleven nodes in Fig. 3(d) for the two networks to be pinning controlled at time t_k, with parameters $\delta = 0.2$ and $\delta = 0.367$. From the conditions of the Theorem 1, we have,

(1)$\|f_{x_i}(\mathbf{x})\|^2 \leqslant l_1\|e_\mathbf{x}\|^2 = 2\|e_\mathbf{x}\|^2$ and $\|f_{y_i}(y)\|^2 \leqslant l_2\|e_\mathbf{y}\|^2 = 1 \cdot \|e_\mathbf{y}\|^2$ for the network in Fig. 3(a), so the condition (1) of Theorem 1 is satisfied. Then $M = 62$, $0 < \Delta_1 < 0.000624$.

(2)$\|f_{x_i}(\mathbf{x})\|^2 \leqslant l_1\|e_\mathbf{x}\|^2 = 4\|e_\mathbf{x}\|^2$ and $\|f_{y_i}(y)\|^2 \leqslant l_2\|e_\mathbf{y}\|^2 = 4 \cdot \|e_\mathbf{y}\|^2$ for the network of Fig. 3(d), so that $M = 247$ and $0 < \Delta_2 < 0.0003$.

For the network in Fig. 3(a), when the pinning impulse interval is taken as $\Delta_1 = 0.0005s$, the nodes achieve synchronization with the leader node, as shown is Fig. 5.

Figure 6(a) shows the state variables of the network in

Fig. 3(d) without the control, which is obviously nonsynchronous. In Figs. 6(b),(c),(d), the 30-node network are successfully driven to synchronize with the leader node $s(t)$ by univariate impulse pinning control with impulse interval $\Delta_2 = 0.0003s$.

In general, to achieve synchronization, the smaller impulse interval and the larger duty ratio correspond to the need for a smaller impulse amplitude. Therefore, in the application, we can adjust the impulse amplitude according to the Theorem derived in the paper to avoid the saturation of the actuator or the saturation of the state variable. In practice, we have used electronic circuit to implement the impulse control in the Chen circuit[16], where the saturation problem was avoided.

In the simulation results of Fig. 5 and Fig. 6, all initial state variables of the network are randomly chosen in [-1,1]. We impose univariate impulse controllers to determine the pinning nodes in the two networks. It is shown that the trajectories of the error are stabilized at zero, which validate the correctness of the proposed method.

Note that, the time delay not only increases the dimension of the original system without time delay, but also brings more and larger positive Lyapunov exponents. It causes the dynamics of the original system to be more complicated. The simulations have demonstrated that the number of positive Lyapunov exponents increases when the time delay τ and time delay gain $\mathbf{C}$ are increased[34,35]. Moreover, the synchronization time is longer than that of the original system, the synchronization being harder to be achieved.

V. CONCLUSION

In this paper, using Lyapunov stability theory, a Theorem is stated and proved, establishing the sufficient condition for network synchronization with univariate impulse pinning control. Numerical simulations are given to demonstrate the validity of the proposed univariate impulse pinning controller.

Note that, some states of the nodes are not observable. But, for the proposed method, one just needs one variable of the oscillator to be observable in order to establish the univariate state feedback controller to synchronize the whole network, instead of the full-state feedback controller, which gives better adaptability and application potential to the proposed method.

ACKNOWLEDGMENTS

This paper was supported in part by the Shaanxi Provincial Special Support Program for Science and Technology Innovation Leader.

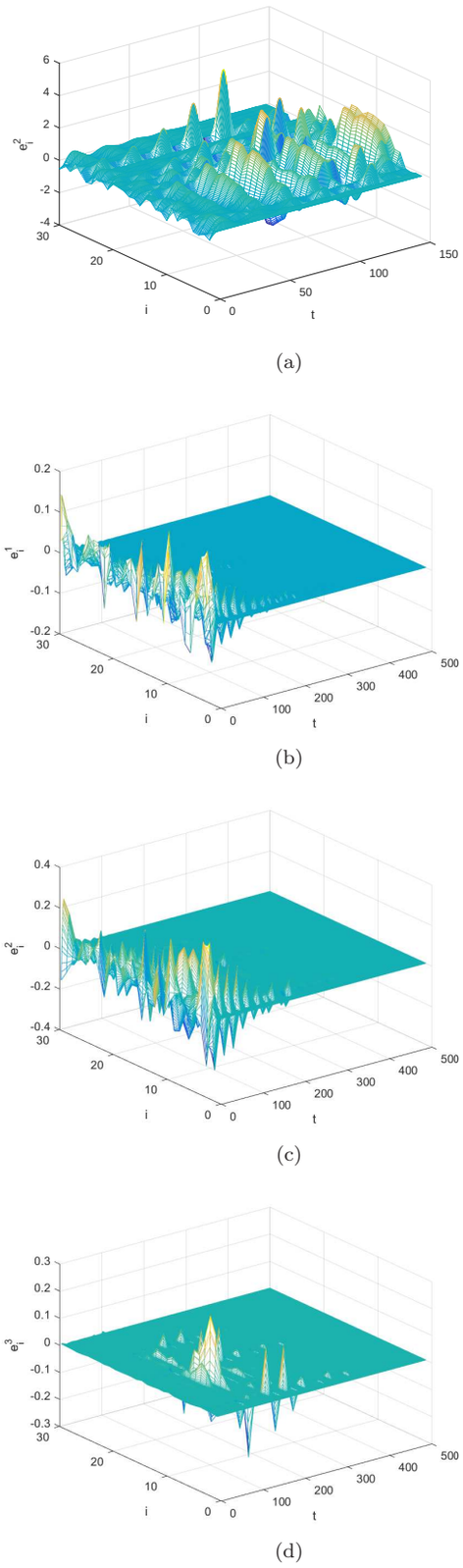

FIG. 6. Synchronization errors e_i^1, e_i^2 and e_i^3 of the network, Eq. (24), in Fig. 1(d); (a) the second state variable error e_i^2 of the network without control; (b), (c) and (d) are the state variables errors e_i^1, e_i^2 and e_i^3 with the univariate impulse pinning control on y, where i indicates the node index.

AIP PUBLISHING DATA SHARING POLICY

The data that support the findings of this study are available from the corresponding author upon reasonable request.

[1]L. Pavel, *Dynamics and stability in optical communication networks: A system theory framework*, Automatica, vol. 40, no. 8, pp. 1361-1370, 2004.
[2]C. Bai, H. P. Ren, G. Kolumbán, *Double-sub-streams M-ary Differential Chaos Shift Keying Wireless Communication System using Chaotic Shape-Forming Filter*, IEEE Trans on Circuits and System I: regular paper, 2020.(early access) Doi:10.1109/TCSI.2020.2993674
[3]Y. Zhang, A. G. Chen, Y. J. Tang, J. W. Dang, G. P. Wang, *Plaintext-related image encryption algorithm based on perceptron-like network*, Information Sciences, vol. 526, pp. 180-202, 2020.
[4]H. P. Ren, Z Ma, *License Plate Recognition Using Complex Network Feature*, in Proceeding of The 11th World Congress on Intelligent Control and Automation, Shenyang, China (2014), pp. 5426 - 5431.
[5]H. P. Ren, C. Bai, M. S. Baptista, C. Grebogi, *Weak connections form an infinite number of patterns in the brain*, Scientific Reports, vol. 7, pp. 46472, 2017.
[6]R. O. Grigoriev, M.C. Cross, H.G. Schuster, *Pinning control of spatiotemporal chaos*, Physical Review Letters, vol. 79, pp. 2795-2798, 1997.
[7]C. D. Li, X. F. Liao, X. F. Yang, *Impulsive stabilization and synchronization of a class of chaotic delay systems*, Chaos, vol. 15, pp. 043103, 2005.
[8]D. Ding, Z. Tang, Y. Wang, Z. C. Ji, *Synchronization of nonlinearly coupled complex networks: Distributed impulsive method*, Chaos, Solitons & Fractals, vol. 133, pp. 109620, 2020.
[9]H. P. Ren, C. Z. Han, *Parameter identification and synchronization of chaotic system using conjugate gradient method*, Chinese Journal of Scientific Instrument, vol. 29, pp. 792, 2008.
[10]J. Zhou, J. A. Lu, J. H. Lv, *Pinning adaptive synchronization of a general complex dynamical network*, Automatica, vol. 44, pp. 996-1003, 2008.
[11]X. S. Yang, J. D. Cao, Z. C. Yang, *Synchronization of couple reaction-diffusion neural network with time-varying delays via pinning-impulsive controller*, SIAM Journal on Control and Optimization, vol. 51, pp. 3486-3510, 2013.
[12]W. L. He, F. Qian, J. D. Cao, *Pinning-controlled synchronization of delayed neural networks with distributed-delay coupling via impulsive control*, Neural Networks, vol. 85, pp. 1-9, 2016.
[13]C. B. Yi, C. Xu, J. W. Feng, J. Y. Wang, Y. Zhao, *Pinning synchronization for reaction-diffusion neural networks with delays by mixed impulsive control*, Neurocomputing, vol. 339, pp. 270-278, 2019.
[14]J. Q. Lu, Z. D. Wang, J. D. Cao, D. W. C. Ho, J. Kurths, *Pinning impulsive stabilization of nonlinear dynamical networks with time-varying delay*, International Journal of Bifurcation and Chaos, vol. 22, pp. 1250176, 2012.
[15]T. P. Chen, X. W. Liu, W. L. Lu, *Pinning complex networks by a single controller*, IEEE Transactions on Circuits and Systems-I, vol. 54, pp. 1317-1326, 2007.
[16]K. Tian, C. Bai, H. P. Ren, C. Grebogi, *Hyperchaos synchronization using univariate impulse control*, Physical Review E, vol. 100, pp. 052215, 2019.
[17]O. E. Rössler. *An equation for hyperchaos*, Physics Letters A, vol. 71, pp. 155-157, 1979.
[18]R. Thomas, V. Basios, M. Eiswirth, T. Kruel, O. E. Rössler, *Hyperchaos of arbitrary order generated by a single feedback circuit, and the emergence of chaotic walks*, Chaos, vol. 14, pp. 669-674, 2004.
[19]X. Q. Wu, Q. S. Li, C. Y. Liu, J. Liu, C. W. Xie, *Synchronization in duplex network of coupled Rössler oscillators with different inner-coupling matrices*, Neurocomputing, 2019. (in press)
[20]I. Bodale, V. A. Oancea, *Chaos control for Willamowski-Rössler model of chemical reactions*, Chaos, Solitons & Fractals, vol. 78, pp. 1-9, 2015.
[21]Q. D. Li, *A topological horseshoe in the hyperchaotic Rössler attractor*, Physics Letters A, vol. 372, pp. 2989-2994, 2008.
[22]K. Tian, H. P. Ren, C. Bai, *Synchronization of hyperchaos with time delay using impulse control*, IEEE Access, vol. 8, pp. 72570-72576, 2020.
[23]H. W. Kuhn, *The Hungarian method for the assignment problem*, Naval Research Logistics Quarterly, vol. 2, pp. 83-97, 1955.
[24]J. Munkres, *Algorithms for Assignment and Transportation Problems*, Journal of Society for Industrial and Applied Mathematics, vol. 5, pp. 32-38. 1957.
[25]K. Pyragas, *Continuous control of chaos by self-controlling feedback*, Physics Letters A, vol. 170, pp. 421-428, 1992.
[26]H. P. Ren, D. Liu, C. Z. Han, *Anticontrol of Chaos via Direct Time Delay Feedback*, Acta Physica Sinica, vol.6 pp. 2694, 2006.
[27]X. Z. Liu, G. Ballinger, *Uniform asymptotic stability of impulsive delay differential equation*, Computers and Mathematics with Application, vol. 41, pp. 903-915, 2001.
[28]L. A. Aguirre, C. Letellier, *Controllability and synchronizability: Are they related?*, Chaos, Solitons and Fractals, vol. 83, pp. 242-251, 2016.
[29]Y. Y. Liu, J. J. Slotine, A. L. Barabasi, *Controllability of Complex networks*, Nature, vol. 473, pp. 167-173, 2011.
[30]C. T. Lin, *Structural Controllability*, IEEE Transactions on Automatic Control, vol. 19, pp. 201-208, 1974.
[31]C. Letellier, I. Sendiña-Nadal, L. A. Aguirre. *A nonlinear graph-based theory for dynamical network observability*, Physical Review E. vol. 98, pp. 020303, 2018.
[32]R. Hermann, A. J. Krener. *Nonlinear Controllability and Observability*, IEEE Transactions on Automatic Control, vol. 22, pp. 728-740, 1977.
[33]H. P. Ren, C. Bai, K. Tian, C. Grebogi. *Dynamics of delay induced composite multi-scroll attractor and its application in encryption*, International Journal of Non-Linear Mechanics, vol. 94, pp. 334-342, 2017.
[34]J. D. Farmer. *Chaotic Attractors of an infinite-dimensional dynamical system*, Physica D: Nonlinear Phenomena, vol. 4, pp. 366 -393, 1982.
[35]P. Grassberger, I. Procaccia. *Measuring the Strangeness of Strange Attractors*, Physica D: Nonlinear Phenomena, vol. 9, pp. 189-208, 1983.

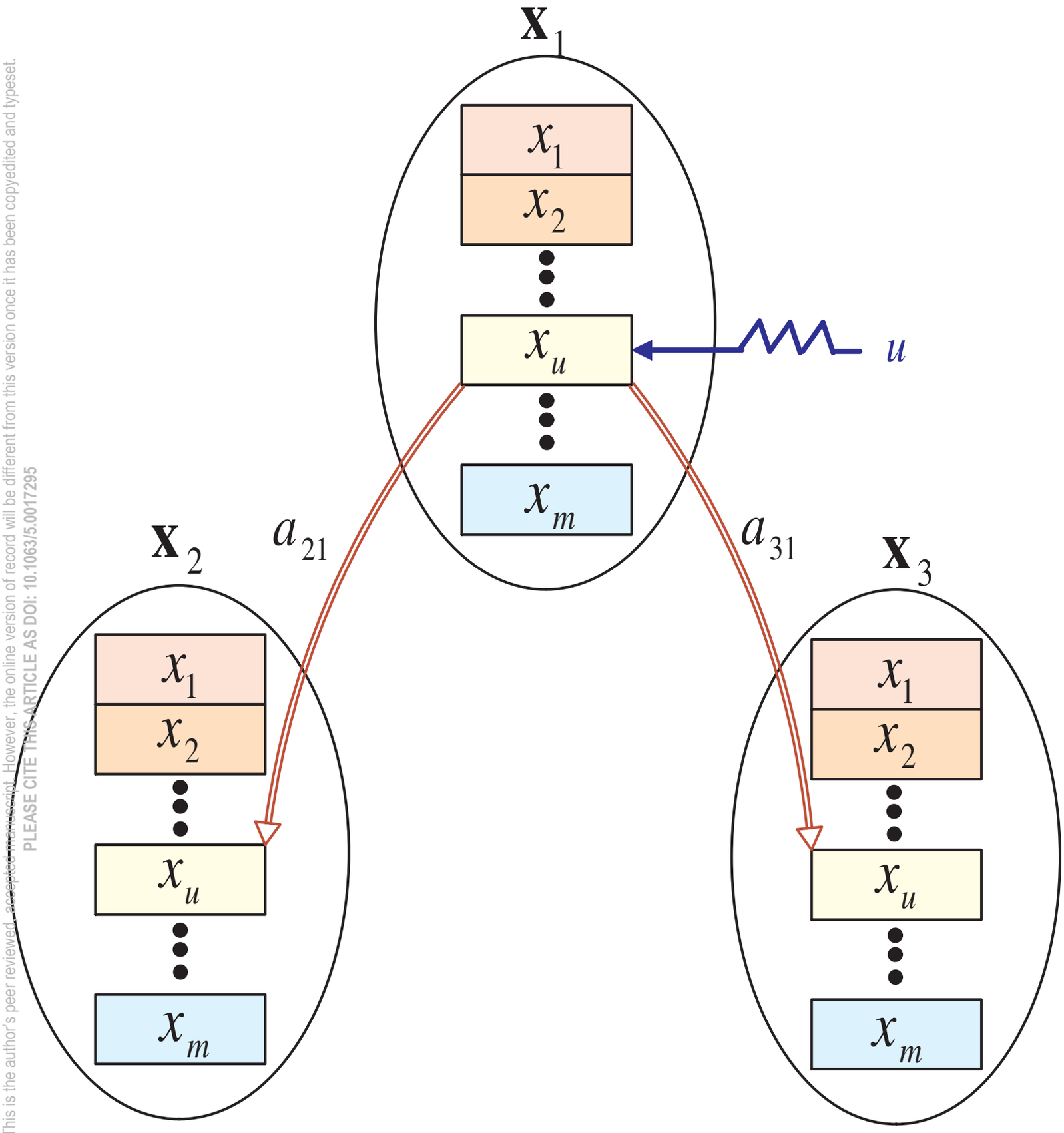

Chaos

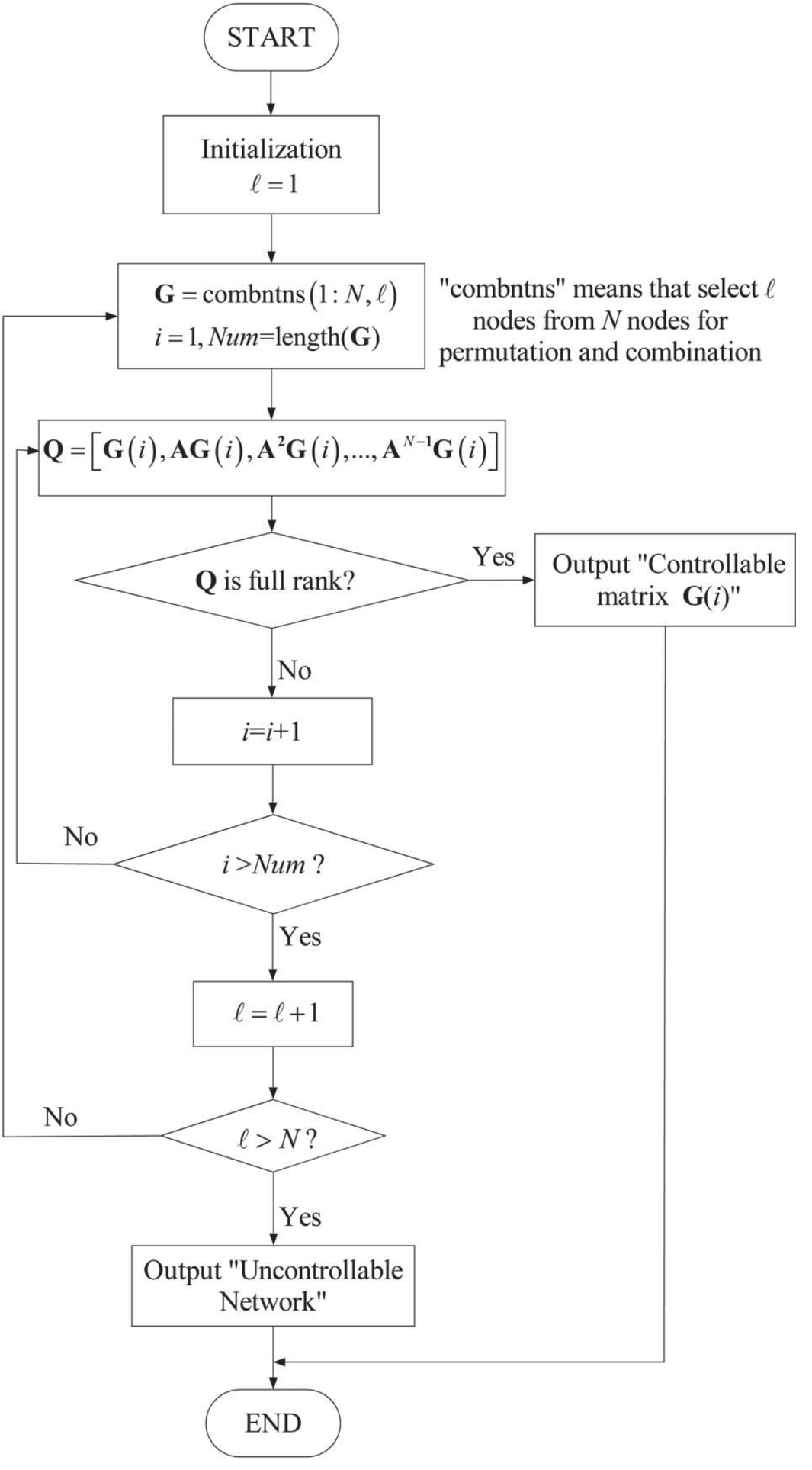

PLEASE CITE THIS ARTICLE AS DOI: 10.1063/5.0017295

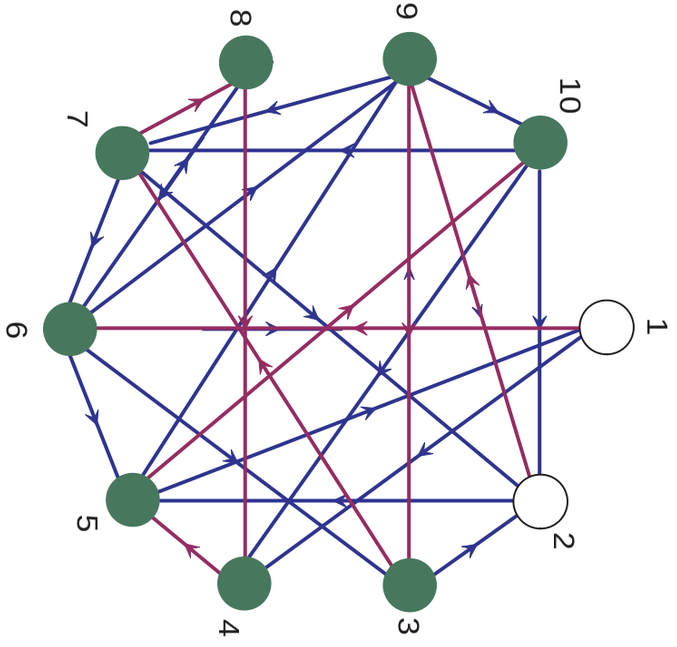

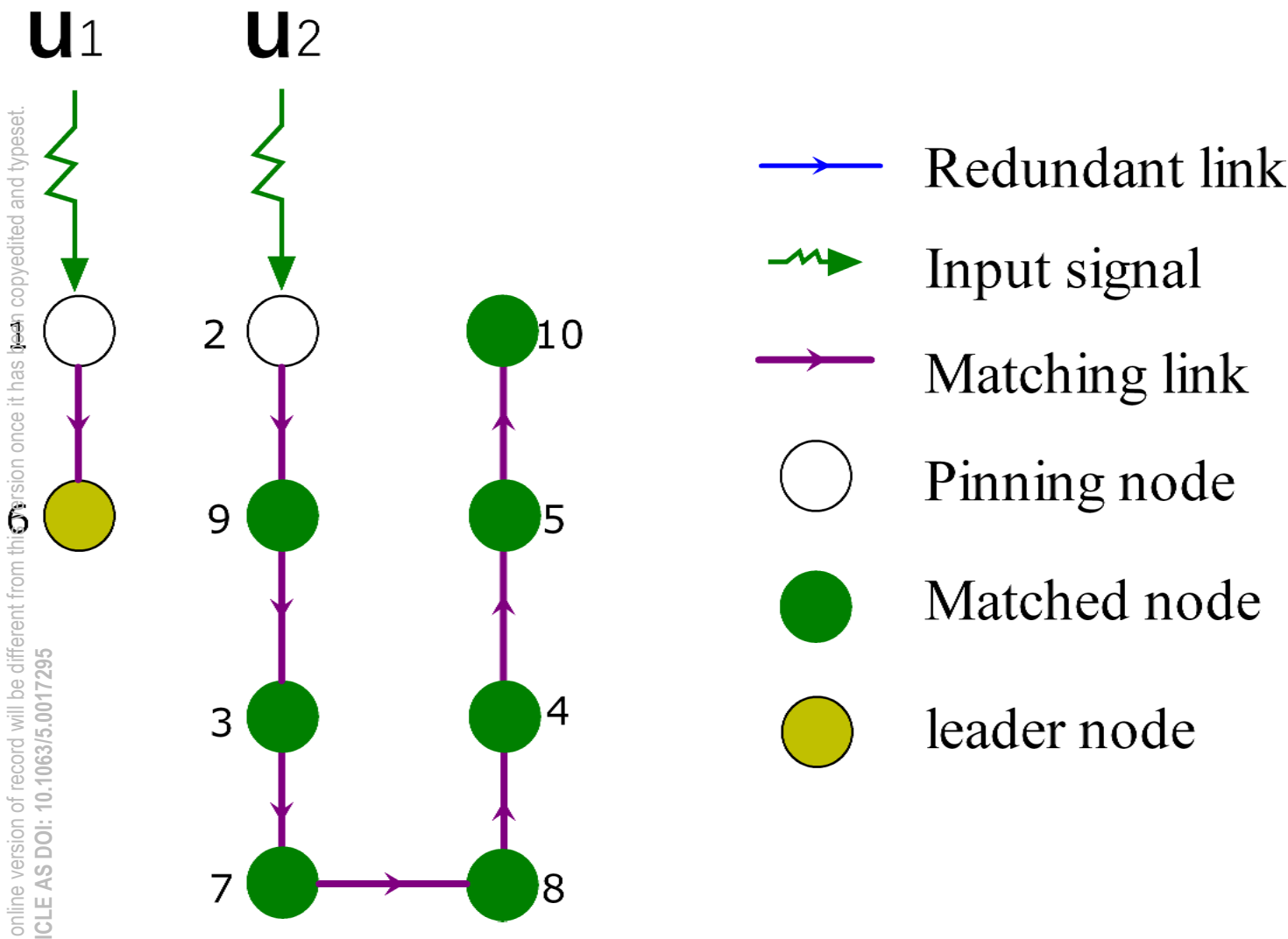

PLEASE CITE THIS ARTICLE AS DOI: 10.1063/5.0017295

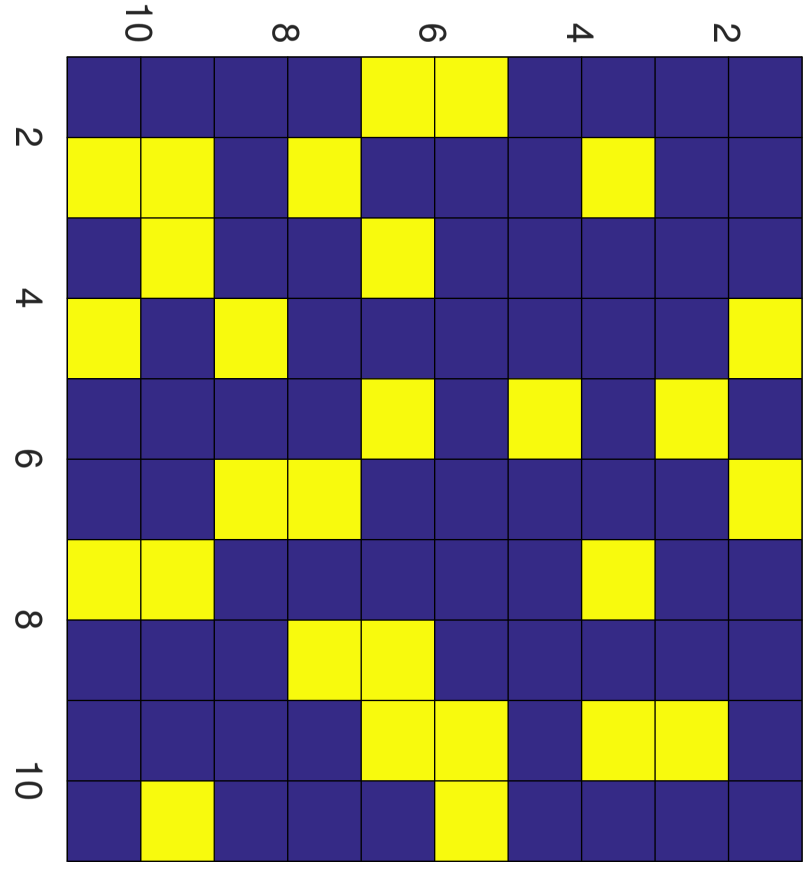

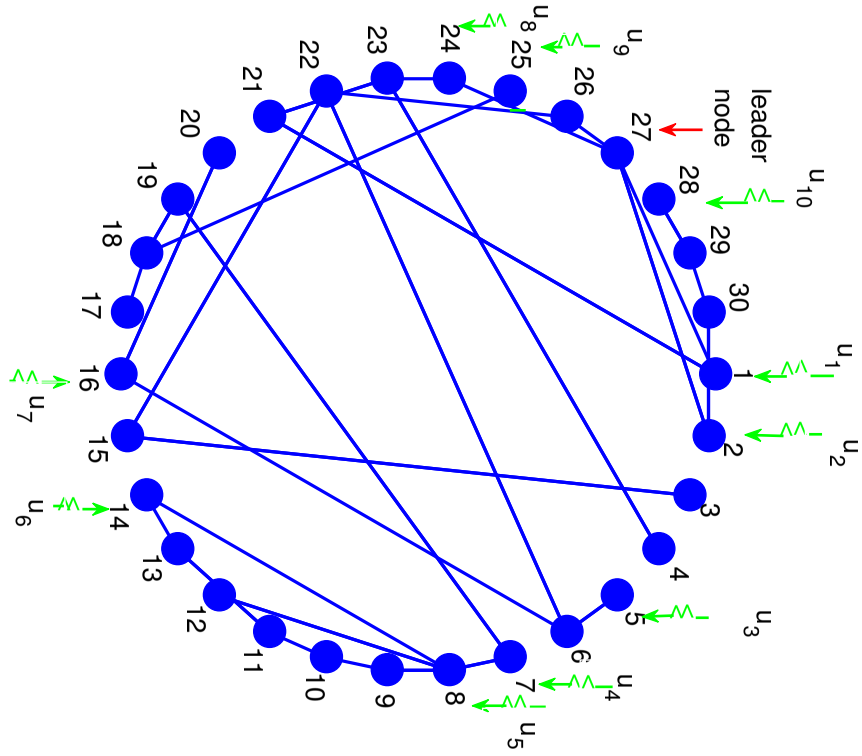

PLEASE CITE THIS ARTICLE AS DOI: 10.1063/5.0017295

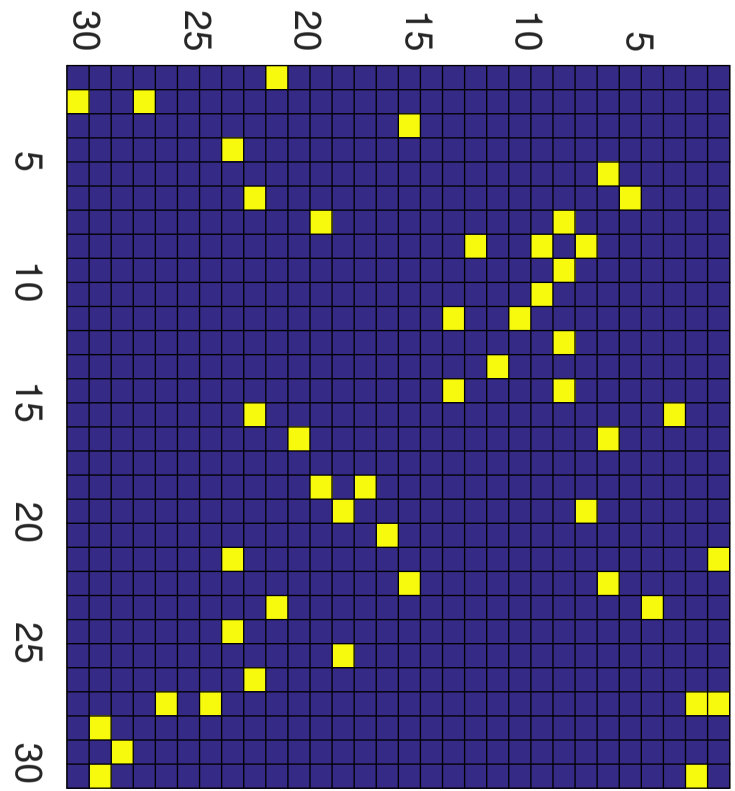

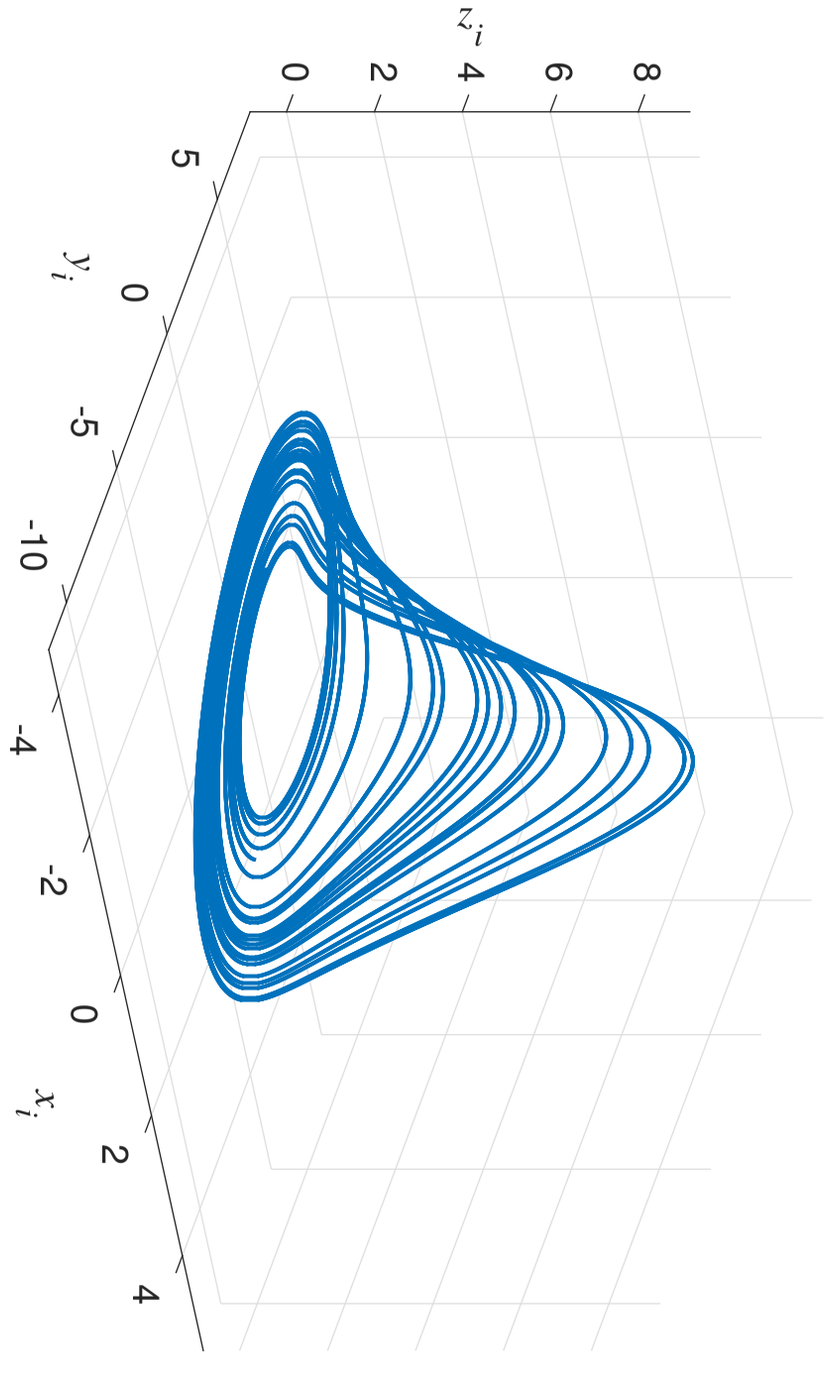

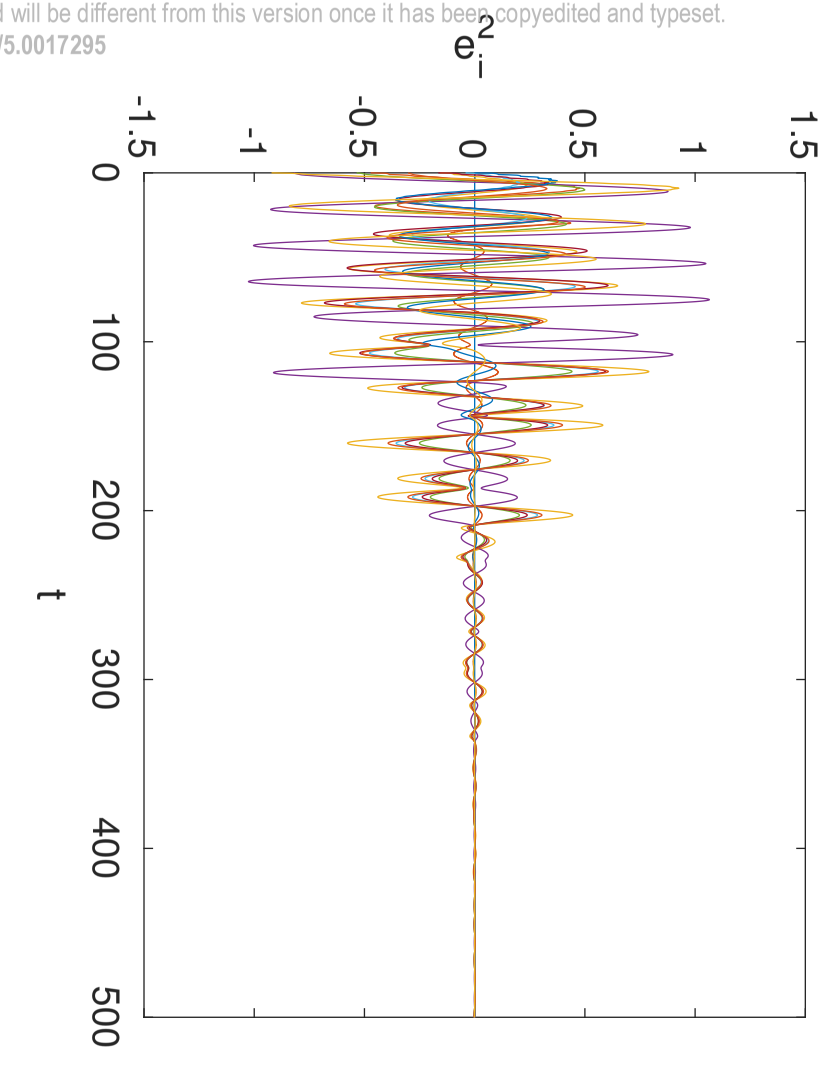

PLEASE CITE THIS ARTICLE AS DOI: 10.1063/5.0017295

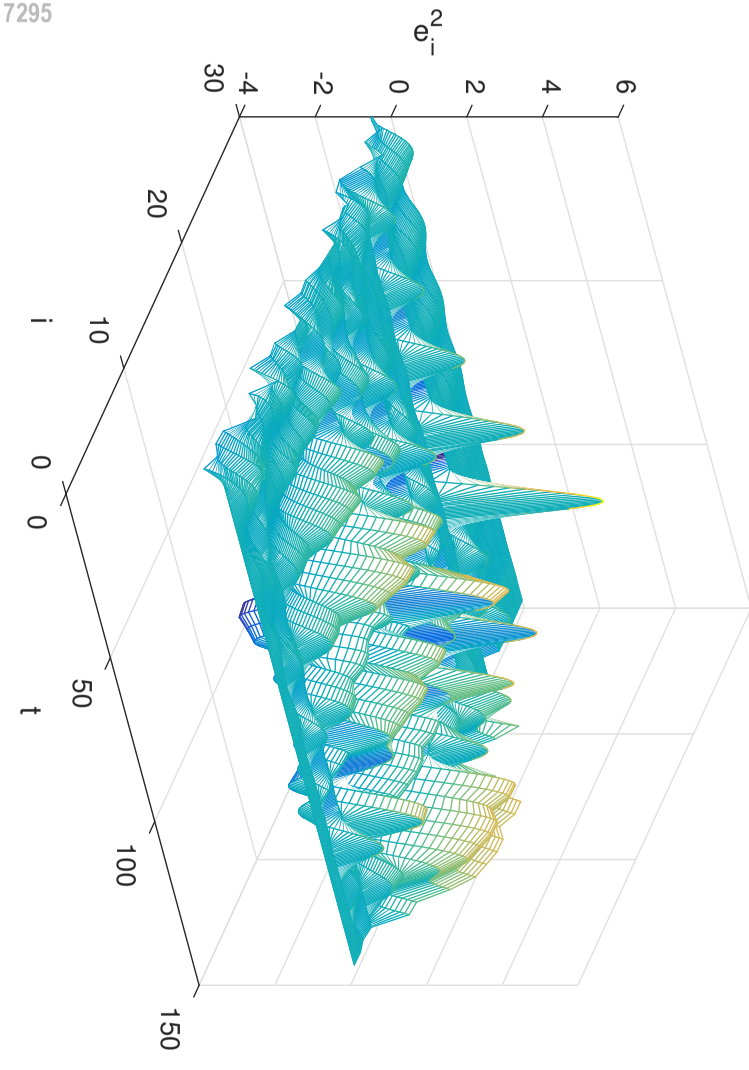

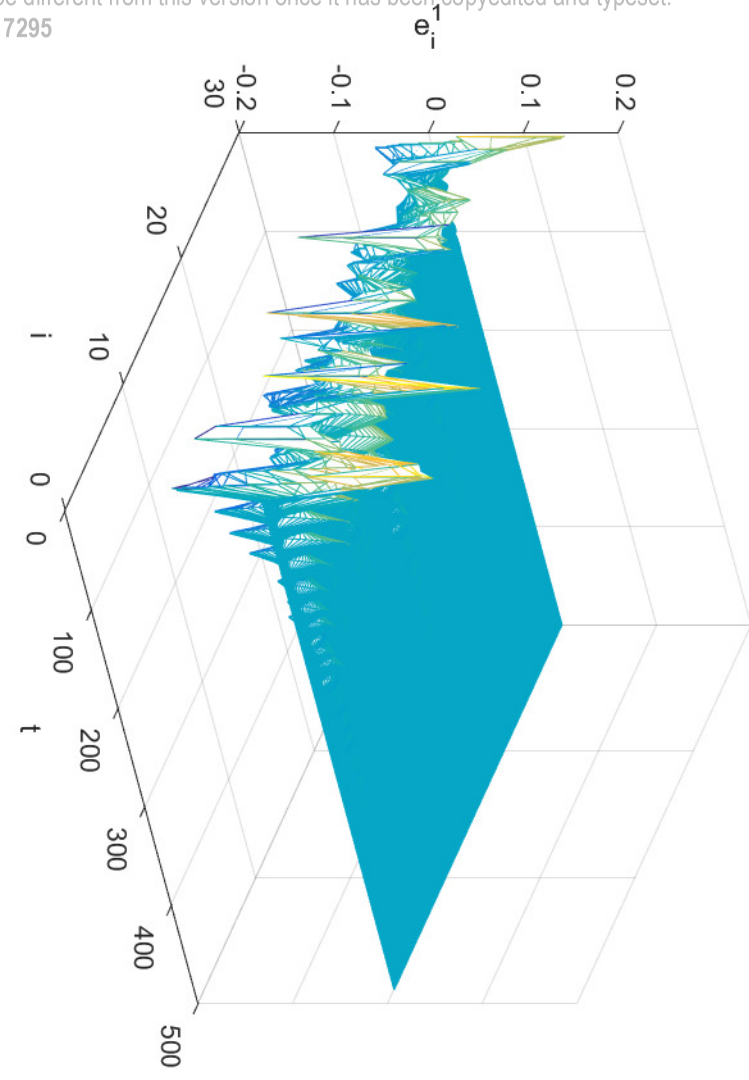

PLEASE CITE THIS ARTICLE AS DOI: 10.1063/5.0017295